

RESEARCH ARTICLE

Modeling the Effects of Morphine on Simian Immunodeficiency Virus Dynamics

Naveen K. Vaidya^{1,2*}, Ruy M. Ribeiro³, Alan S. Perelson³, Anil Kumar²

1 Department of Mathematics and Statistics, University of Missouri-Kansas City, Missouri, United States of America, **2** Division of Pharmacology, School of Pharmacy, University of Missouri-Kansas City, Missouri, United States of America, **3** Theoretical Biology and Biophysics Group, Los Alamos National Laboratory, Los Alamos, New Mexico, United States of America

* vaidyan@umkc.edu



OPEN ACCESS

Citation: Vaidya NK, Ribeiro RM, Perelson AS, Kumar A (2016) Modeling the Effects of Morphine on Simian Immunodeficiency Virus Dynamics. *PLoS Comput Biol* 12(9): e1005127. doi:10.1371/journal.pcbi.1005127

Editor: Becca Asquith, Imperial College London, UNITED KINGDOM

Received: February 16, 2015

Accepted: August 25, 2016

Published: September 26, 2016

Copyright: This is an open access article, free of all copyright, and may be freely reproduced, distributed, transmitted, modified, built upon, or otherwise used by anyone for any lawful purpose. The work is made available under the [Creative Commons CC0](https://creativecommons.org/licenses/by/4.0/) public domain dedication.

Data Availability Statement: All relevant data are within the paper and its Supporting Information files.

Funding: This work was funded by a UMRB grant KDA-91 (NKV) from the University of Missouri Research Board, the NSF grant DMS-1616299 (NKV), and start-up funds from the University of Missouri – Kansas City (NKV). Portions of this work were done under the auspices of the US Department of Energy under contract DE-AC52-06NA25396 and supported by NIH grants R01-AI028433 and R01-AI104373, and the National Center for Research Resources and the Office of Research Infrastructure Programs (ORIP) through grant R01-OD011095

Abstract

Complications of HIV-1 infection in individuals who utilize drugs of abuse is a significant problem, because these drugs have been associated with higher virus replication and accelerated disease progression as well as severe neuropathogenesis. To gain further insight it is important to quantify the effects of drugs of abuse on HIV-1 infection dynamics. Here, we develop a mathematical model that incorporates experimentally observed effects of morphine on inducing HIV-1 co-receptor expression. For comparison we also considered viral dynamic models with cytolytic or noncytolytic effector cell responses. Based on the small sample size Akaike information criterion, these models were inferior to the new model based on changes in co-receptor expression. The model with morphine affecting co-receptor expression agrees well with the experimental data from simian immunodeficiency virus infections in morphine-addicted macaques. Our results show that morphine promotes a target cell subpopulation switch from a lower level of susceptibility to a state that is about 2-orders of magnitude higher in susceptibility to SIV infection. As a result, the proportion of target cells with higher susceptibility remains extremely high in morphine conditioning. Such a morphine-induced population switch not only has adverse effects on the replication rate, but also results in a higher steady state viral load and larger CD4 count drops. Moreover, morphine conditioning may pose extra obstacles to controlling viral load during antiretroviral therapy, such as pre-exposure prophylaxis and post infection treatments. This study provides, for the first time, a viral dynamics model, viral dynamics parameters, and related analytical and simulation results for SIV dynamics under drugs of abuse.

Author Summary

The HIV epidemic continues to be a severe public health problem within the USA and many parts of the world. A substantial number of HIV-infected individuals are intravenous drug users who abuse opiates. Drugs of abuse lead not only to high HIV transmission, but also to high viral load, increased disease progression, and augmented HIV-associated neurocognitive disorder in HIV-1 infected individuals. In this study, using a

(ASP). AK acknowledges the support from NIDA (grant number DA015013). The funders had no role in study design, data collection and analysis, decision to publish, or preparation of the manuscript.

Competing Interests: The authors have declared that no competing interests exist.

novel mathematical model and experimental data from macaques, we evaluate some important effects of morphine, an active metabolite of heroin, on simian immunodeficiency virus (SIV) dynamics. In particular, we quantify the morphine-induced target cell subpopulation switch that results in a high proportion of target cells with higher susceptibility to SIV infection. Consistent with experimental observations, our results reveal that morphine promotes increased co-receptor expression, which can increase the rate of target cell infection. This in turn may explain the observation that HIV infected individuals with drugs of abuse may suffer from higher viral load, higher CD4 count loss, a larger basic reproduction number, and higher probability of failing antiretroviral therapy. Our model and results may be useful to formulate guidelines on incorporating extra efforts needed to manage HIV infection in drug abusers.

Introduction

Drug abuse is one of the leading causes for transmission of human immunodeficiency virus (HIV) within the USA, and in many parts of the world [1–3]. Since the beginning of the HIV epidemic, injection drug use (IDU) has contributed more than one-third (36%) to the total AIDS cases in the United States [4]. HIV-1 infected patients often suffer from HIV-associated neurocognitive disorder (HAND), which has been substantially linked with drug abuse [3, 5]. Contaminated needle sharing and increased risky sexual behavior among injection drug users put them at a higher risk of getting infected with HIV and at a greater chance of developing neurological abnormalities [6–8]. The dependence of many HIV-infected patients on drugs of abuse, such as opiates, is a significant problem in the post-HAART era [3]. Despite being a considerable problem for both science and society, the mechanism by which drug abuse contributes to HIV infection and pathogenesis is not well understood and it is important to study how drugs of abuse affect HIV dynamics.

Opiate addictions often include many uncertain factors such as variable poly-drug abuse, inconsistent drug dosing, poor subject health, risky sexual behavior, variable stressful environment, and the use of other illicit substances [9]. As a result of such extreme complexity of the opiate addiction, studies on HIV infection combined with opiate addictions have reached contrasting conclusions, including no effects, adverse effects, and survival advantages for those engaged in opiate abuse [10–14].

Better understanding of the effects of drugs of abuse, such as morphine, on viral pathogenesis and disease progression has been provided by the development of experimental nonhuman primate models of IDU and HIV disease that utilize simian immunodeficiency virus (SIV) and simian human immunodeficiency virus (SHIV) in rhesus macaques [3, 15–17]. The experiments utilizing these animal models along with other in-vitro experiments demonstrate considerable effects of morphine on viral dynamics, immune responses, and virus evolution [3, 15–20]. Combined these experiments strongly support the hypothesis that morphine enhances HIV-1/SIV infectivity as well as HAND.

Mathematical models have significantly contributed to our understanding of virus and immune cell dynamics [21–24], and may become valuable in understanding HIV infection dynamics under drugs of abuse. Here, we develop a novel viral dynamic model with the main objective of studying whether a model based on the experimental observation that morphine upregulates the expression of SIV/HIV co-receptors [25–27] can explain the effect of morphine on SIV viral load kinetics in morphine-dependent SIV-infected macaques. We show that our model agrees well with viral load and CD4+ T-cell count data from both morphine-dependent

and control macaques infected intravenously with a mixture of SHIV and SIV. Using our model, we evaluate the role of morphine in altering target cell susceptibility, viral dynamics, steady-state viral load, the loss of CD4 cells, and the effectiveness of antiretroviral therapy (ART). We further discuss how morphine can increase the basic reproduction number, causing further obstacles for HIV prophylaxis.

Materials and Methods

Ethics Statement

Rhesus macaques used for the study were obtained from the Caribbean Research Primate Center and housed in the Animal Resource Center of the University of Puerto Rico, San Juan. The experimental protocol was approved by the Institutional Animal Care and Use Committee, and the research was performed in accordance with the Guide for the Care and Use of Laboratory Animals.

Experiment and Data

Viral load and CD4 count data were obtained from 12 male rhesus macaques (*Macaca mulatta*) [16]. The animals were confirmed negative for simian T-cell leukemia virus type 1 and simian retrovirus. The animals were divided into two groups: morphine-dependent (6 animals) and control (6 animals). The morphine-dependent environment was created and maintained by injecting intramuscularly three daily 1–5 mg/kg doses of morphine for 2 weeks, followed by three daily 5 mg/kg doses for an additional 18 weeks. The same amount of normal saline at the same time was given to control animals. All macaques were infected intravenously with a 2-ml inoculum containing 10^4 TCID₅₀ doses each of SHIV_{KU-1B}, SHIV_{89.6p}, and SIV 17E-Fr. These animals were monitored for a period of 12 weeks, and the plasma viral load and CD4 count were measured at weeks 0, 1, 2, 3, 4, 6, 8, 10, and 12 post infection as described in Kumar et al. [16]. The morphine-dependent animals were maintained on morphine throughout the observation period. The experimental data are given in Table 1.

Model

We incorporate experimentally observed morphine effects into the basic model of viral infection that has been used previously to describe acute infection in both HIV infected humans and SIV infected macaques [28–33]. We focus on modeling acute infection dynamics during the first 84 days post infection, when viral load and CD4+ T cell counts were obtained from the experimentally infected macaques. During the early period, neutralizing antibodies specific to any of the SIV strains were not detected (Kumar's Lab). Further, during this period, no significant difference in antibody and CD8+ T-cell levels were found between the morphine-dependent and control animal groups (Kumar's Lab). Thus, while immune effects may occur during this early period [34], and some viral kinetic models of acute infection have included immune responses [35–40], the available data suggests that they are not responsible for the difference in viral dynamics between the morphine-dependent and control group. For this reason, as well as the fact that target cell limited models have been shown to agree well with viral load data collected during acute infection, we choose as our base model a target cell limited model, as done in previous studies of acute infection [28–32]. However, we also examined alternative explanations based on an effect of morphine on the immune response.

The direct correlation between morphine dependence and viral replication has been attributed to the increased expression of chemokine receptors, such as CCR5 and CXCR4, on lymphocytes and other cells [3, 26, 27, 41]. To successfully infect target cells, HIV requires co-

Table 1. Viral loads (vRNA copies/ml) and CD4 counts (CD4 cells per μ l) for individual monkeys (Morphine group: M1-M6; Control group: C1-C6).

Animal		Wk 0	Wk 1	Wk 2	Wk 3	Wk 4	Wk 6	Wk 8	Wk 10	Wk 12
M1	VL		6.67e5	4.93e6	4.79e4	1.20e5	4.79e4	3.47e5	4.85e6	4.01e6
	CD4	852	133	45	24	45	57	6	10	16
M2	VL		7.83e5	3.57e7	8.63e5	2.03e5	3.55e5	4.95e5	1.65e6	2.03e7
	CD4	1373	617	185	56	36	9	9	21	6
M3	VL		1.52e7	1.81e7	5.10e5	6.40e5	5.10e5	1.60e7	7.32e6	2.59e7
	CD4	1193	164	34	17	22	128	4	7	39
M4	VL		3.55e6	2.41e6	3.08e5	1.36e5	2.10e4	2.3e3	5.6e3	1.4e3
	CD4	1263	77	422	243	274	552	676	687	707
M5	VL		1.67e7	7.46e6	2.95e6	3.12e5	4.64e5	2.46e5	1.92e5	4.06e5
	CD4	1316	43	65	112	440	29	25	31	42
M6	VL		5.29e6		2.12e5	2.80e5	5.26e5	5.08e4	1.89e5	1.28e5
	CD4	1281	191	16	5	5	137	4	8	31
C1	VL		7.57e6	8.96e6	5.89e5	8.32e5	2.75e5	9.84e4	2.25e5	3.14e4
	CD4	1567	609	399	175	536	469	448	656	334
C2	VL		2.03e7	2.79e6	9.20e4	9.70e4	1.13e5	7.50e4	9.5e4	8.70e4
	CD4	1779	453	247	49	70	150	191	369	113
C3	VL		1.29e6	1.55e7	3.29e6	3.37e5	1.86e5	9.10e4	4.8e4	1.4e4
	CD4	751	340	559	55	110	98	102	135	154
C4	VL		1.38e7	1.44e7	8.32e5	7.32e5	6.49e5	4.22e5	4.22e5	2.56e5
	CD4	671	665	315	380	410	380	445	448	510
C5	VL		4.04e6	2.03e7	3.19e5	1.50e5	8.00e4	5.50e4	3.30e4	7.00e3
	CD4	1642	765	400	169	188	231	263	294	264
C6	VL		4.06e6	5.66e6	3.77e5	1.42e5	3.34e5	2.03e5	1.07e5	1.75e5
	CD4	1414	885	307	82	101	119	171	373	102

doi:10.1371/journal.pcbi.1005127.t001

receptors, mainly CCR5 or CXCR4, along with CD4 receptors [42, 43]. HIV infectivity, as measured by HIV p24 levels, is proportional to co-receptor expression [44]. Experimental studies have clearly demonstrated that morphine increases CCR5 and CXCR4 expression on various cell types [26, 27, 41, 45, 46], and can lead to higher set-point viral loads [16]. Combined, these experimental results suggest that morphine by inducing HIV co-receptor expression on target cells increases the susceptibility of these cells to HIV infection, resulting in higher viral replication. We note that there has been limited study of co-receptor expression *in vivo* under morphine conditioning. Thus the objectives of this study are to model the hypothesis that morphine increases CCR5 expression, to test this hypothesis in a quantitative manner and to see if it yields a model that fits *in vivo* data.

Based on *in vitro* observations about the effects of morphine conditioning on CCR5 levels, we develop a model containing two subpopulations of target cells (CD4⁺ T cells)—one with lower susceptibility to infection (i.e. lower infection rate) due to a low level of co-receptor expression, T_l , and another with higher susceptibility (i.e. higher infection rate) due to a high level of co-receptor expression, T_h . Levels of co-receptor expression could more accurately be described by considering many subpopulations of target cells, but the data we analyze lacks such precision, so we opted for this simpler approach. Further, as cells become activated and differentiate, co-receptor expression can change. Thus, our model incorporates a base rate at which cells transfer from low expression to high expression. A key hypothesis to be tested is that morphine enhances the rate of cells transferring from the T_l -group to the T_h -group resulting in a higher proportion of T_h cells in the target cell population.

A schematic diagram of the model is presented in Fig 1. We assume that target cells are generated at a constant rate λ and have a per capita net loss rate d , which is the difference between the rate of loss from cell death and rate of gain due to cell division. For simplicity, we assume that newly generated target cells are all in the T_l -group. The rate of transition from T_l to T_h is denoted by r , while that from T_h to T_l is denoted by q . Target cells, T_l and T_h , become productively infected cells, I , upon contact with free virus, V , at rates β_l and β_h , respectively. The parameters δ , p , and c are the rate constants of infected cell loss, virus production by infected cells, and virus clearance, respectively. The model can be described by the following set of equations:

$$\frac{dT_l}{dt} = \lambda + qT_h - dT_l - rT_l - \beta_l VT_l, \quad T_l(0) = T_{l0}, \tag{1}$$

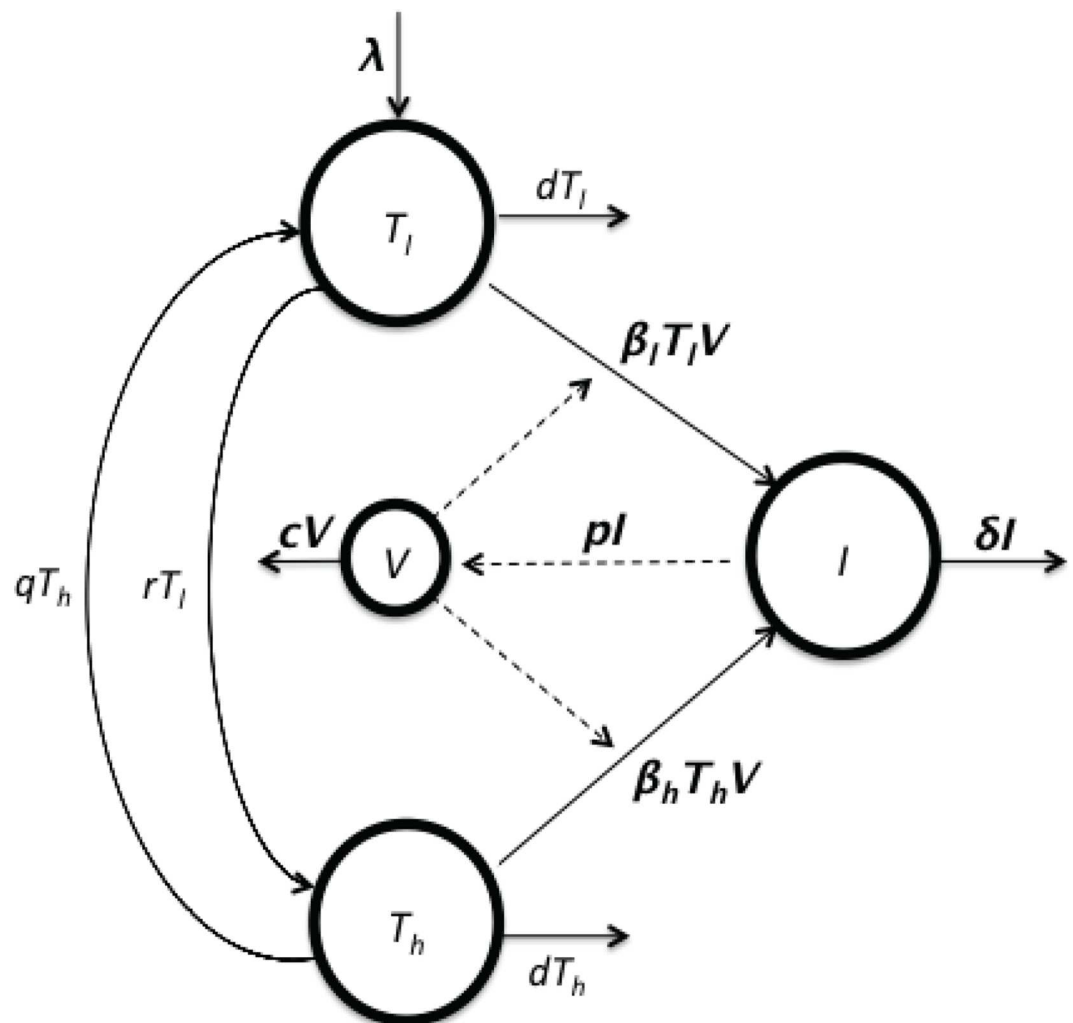


Fig 1. Schematic diagram of the model. The model contains two subpopulations, T_l and T_h , of target cells, with low and high susceptibilities to infection. Cells within these populations can switch susceptibilities with rates r and q , respectively. The target cells are infected, upon contact with virus, V , at rates β_l and β_h , respectively, and become productively infected cells, I .

doi:10.1371/journal.pcbi.1005127.g001

$$\frac{dT_h}{dt} = rT_l - dT_h - \beta_h VT_h - qT_h, \quad T_h(0) = T_{h0}, \quad (2)$$

$$\frac{dI}{dt} = \beta_l VT_l + \beta_h VT_h - \delta I, \quad I(0) = I_0, \quad (3)$$

$$\frac{dV}{dt} = pI - cV, \quad V(0) = V_0. \quad (4)$$

In this model, the total CD4 count is given by $T = T_l + T_h + I$, with $T(0) = T_0$. The change in CD4 count is thus governed by the equation $dT/dt = \lambda - dT - (\delta - d)I$.

As mentioned above, we also examined immune response models (IR). The details of these models are given in [S2 Text](#). In summary, we modified the basic viral dynamics model ($\frac{dT}{dt} = \lambda - dT - \beta VT$, $\frac{dI}{dt} = \beta VT - \delta I$, $\frac{dV}{dt} = pI - cV$), by introducing an equation, $\frac{dE}{dt} = \frac{\lambda E}{K+1} - d_E E$, representing the dynamics of effector cells, E . We then considered two different effects of the immune response on the viral dynamics, namely cytolytic (CIR model) and non-cytolytic (NIR model) effects. We modeled the cytolytic effect by replacing δ by $(\delta + \delta_E E)$, and the non-cytolytic effect by replacing p by $p/(1 + p_E E)$, where δ_E and p_E represent the rate of killing of infected cells (cytolytic) and the rate of reduction of viral production (non-cytolytic) due to cytokines released by effector cells, respectively. We fitted these models to each group of animals separately, as well as to both groups combined, and compared the models using the small-sample (second order) Akaike information criterion [47], AIC_C (see [S2 Text](#)). The smallest AIC_C value obtained among all cases of the CIR and NIR models was 14.97, while the AIC_C value for our target cell population switch (TCS) model is -5.07 (morphine) and -15.59 (control). Moreover, the killing rate $\delta_E E$ predicted by the CIR model is always smaller than δ , and the factor $p_E E$ predicted by NIR model is much smaller than 1, indicating that the putative effects of the immune response effects are negligible. In [S2 Text](#) we discuss these immune response models, show the best fit parameters and present the fits to the data.

Parameter Estimation

Since the animals were initially uninfected, we set $I_0 = 0$. As estimated by Ramratnam et al. [48], the virion clearance rate constant during chronic infection in humans varies between 9.1 and 36.0 day^{-1} , with an average of 23 day^{-1} . Results in Zhang et al. [49] indicate that SIV clearance rate from plasma of rhesus macaques is at least as fast. Here, we take $c = 23 \text{ day}^{-1}$ as a minimal estimate and acknowledge that this value might be larger in macaques. Following previous estimates [32], we take 100 days as the life span of uninfected target cells, i.e., $d = 0.01 \text{ day}^{-1}$. Initially, the average CD4 counts in the control and morphine-conditioned animals were 1,366 per μl and 1,213 per μl , respectively. According to the vitro experiment by Steele et al. [41], about 3% of the control cells and about 5% of the morphine treated cells expressed CCR5 in the absence of infection. This allows us to estimate that there are 40,980 and 60,650 CCR5 expressing CD4+ T cells/ml in the absence of infection in this in vitro system. Due to lack of in vivo co-receptor expression data, we take these values as initial estimate of cells with higher CCR5 expression. That is, we take $T_{h0} = 40,980/\text{ml}$, $T_{l0} = T(0) - T_{h0}$ for the control group, and $T_{h0} = 60,650/\text{ml}$, $T_{l0} = T(0) - T_{h0}$ for the morphine group. We also performed a sensitivity analysis on the effect of changing T_{h0} .

Note that as shown by Sachsenberg et al. [50], only a fraction of CD4+ T cells in peripheral blood express activation markers and hence are preferred targets for HIV infection. Based on

this, Stafford et al. [32] chose to use 1% of all CD4⁺ T cells as targets for HIV. However, the fraction of CD4⁺ T cells chosen to be the initial number of target cells, T_0 , does not affect the results of this study because the only parameters affected by a different choice of T_0 are λ and p , and the redefining $T_l \rightarrow T_l/T_0$, $T_h \rightarrow T_h/T_0$, $I \rightarrow I/T_0$, $\lambda \rightarrow \lambda T_0$, and $p \rightarrow p/T_0$ will keep the system unaltered (see S1 Text). The scaled system shows that the estimate of p is related to T_0 as pT_0 appears in the scaled system instead of p . Using the SIV burst size *in vivo* in rhesus macaques as approximately 5×10^4 virions per infected cell [51], an average life-span of productively infected cells of 1 day [52], and the previous estimate of the number of target cells for SIV infection in macaques of 5% of the CD4 count [33], we take $p = 2500 \text{ d}^{-1}$.

The initial viral load, V_0 , needs to be estimated. Each macaque was infected intravenously with a 2-ml inoculum containing 10^4 TCID₅₀ of each of three chosen SIV viruses [16]. The total of 3×10^4 TCID₅₀ of viruses comprises at least 3×10^5 HIV RNA copies [53]. A macaque, on average, weighs 1/10 of a human, which approximately gives 1.5 liter of extracellular water in a macaque. Assuming that the infused virions (RNA copies) are dispersed into extracellular water, the initial viral load, V_0 , can be estimated as $V_0 \approx 3 \times 10^5 / 1.5L \approx 200$ viral RNA copies/ml. Thus we take $V_0 = 200$ viral RNA copies/ml for the base case and perform a sensitivity analysis by varying V_0 from $1 \log_{10}$ to $4 \log_{10}$ viral RNA copies/ml. We estimated the remaining parameters ($\lambda, \beta_b, \beta_h, \delta, r, q$) by fitting the model to experimental data.

Data Fitting

We performed data fitting to each monkey individually. We solved Eqs (1–4) numerically using the Runge-Kutta 4 algorithm in Berkeley Madonna [54]. The predicted \log_{10} values of the viral loads and the CD4 counts were fit to the corresponding log-transformed data via a nonlinear least squares regression method, in which the sum of the squared residuals (SSR), i.e. the difference between the model predictions and the corresponding experimental values, is minimized. SSR is calculated using the following formula:

$$SSR = \sum_{t_v=1}^{N_V} [\log_{10} V(t_v) - \log_{10} \bar{V}(t_v)]^2 + \sum_{t_c=1}^{N_C} [\log_{10} T(t_c) - \log_{10} \bar{T}(t_c)]^2,$$

where $V(t_v)$ represents the viral load at time t_v predicted by the model, $T(t_c)$ represents CD4 count at time t_c predicted by the model, and $\bar{V}(t_v)$ and $\bar{T}(t_c)$ are the corresponding data. N_V and N_C are total number of viral load and CD4 count data points used for fitting, respectively. In our case, a total of 15 to 16 data points are available for each fitting. As the maximum viral load and maximum T cell count per mL were similar we did not weight the two terms on the right-hand side of this equation differently.

We also tried fitting viral load on a \log_{10} scale and CD4 count on a linear scale, but we found that the best-fit parameters were highly dependent on the ratio of weights, applied to the sum of residuals of these two data sets.

Using the set of parameters obtained from Berkeley Madonna as initial guesses, we refined the fit using MATLAB. Finally, for each best-fit parameter estimate, we provide 95% confidence intervals (CI), which were computed from 1000 replicates, by bootstrapping the residuals [55, 56]. We used t-tests to compare the estimated parameters for the two groups of animals.

Results

Based on experimental studies that showed increased levels of CCR5 and CXCR4 expression in various cell types [26, 27, 41, 45, 46] in morphine-dependent animals and a high

correlation between co-receptors expression and the pathogenesis of HIV and SIV infection [41, 57–59], we developed a model to test the hypothesis that morphine increases the susceptibility of target cells to HIV/SIV infection. The model contains two subpopulations of target cells (CD4⁺ T cells) with lower and higher susceptibilities to infection due to different level of co-receptor expression.

Model-Fit to the Data

Estimated parameters obtained by fitting the data from the individual macaques in the morphine group and the control group are given in Table 2 and the corresponding best-fits to the data in each animal are shown in S1 Fig. 95% bootstrap confidence intervals of the estimated parameters are given in S1 Table. In order to make a visual comparison between the viral load kinetics in the two groups of animals more apparent, we plot in Fig 2 the mean log₁₀ viral load and mean CD4 count dynamics for the two groups as well as best-fit curves to the mean data. Consistent with previous experimental results [16], as shown in Fig 2, the model predicts a significantly higher viral load set-point in the morphine group than in the control group. Moreover, morphine dependence may alter various properties related to SIV dynamics, which we analyze in the subsections below, including the variation of these properties among the animals.

Susceptibility of T Cell Subpopulations

In our model we considered two classes of target cells, T_l and T_h , with different susceptibilities to HIV/SIV infection due to different levels of co-receptor expression. We estimated the

Table 2. Estimated Parameters for Individual Monkeys (Morphine group: M1-M6; Control group: C1-C6). Last row for each group represents estimates for the mean log₁₀ viral load and the mean CD4 count.

Monkey	δ day ⁻¹	λ ml/day	r day ⁻¹	q day ⁻¹	β_l ml/day	β_h ml/day
M1	0.36	1.97×10^3	0.62	4.91×10^{-7}	6.15×10^{-9}	7.63×10^{-8}
M2	0.31	2.74×10^3	0.56	4.97×10^{-7}	4.83×10^{-10}	9.60×10^{-8}
M3	0.39	9.42×10^3	0.39	4.83×10^{-6}	5.83×10^{-9}	7.88×10^{-8}
M4	0.62	9.39×10^3	0.70	2.40×10^{-7}	9.79×10^{-9}	1.79×10^{-8}
M5	0.53	3.41×10^3	0.30	4.53×10^{-8}	1.52×10^{-11}	9.81×10^{-8}
M6	0.31	1.47×10^3	0.53	4.64×10^{-8}	5.22×10^{-10}	9.80×10^{-8}
Mean	0.42	4.73×10^3	0.52	1.02×10^{-6}	3.80×10^{-9}	7.75×10^{-8}
Median	0.37	3.08×10^3	0.55	3.66×10^{-7}	3.18×10^{-9}	8.74×10^{-8}
SD	0.12	3.68×10^3	0.15	1.87×10^{-6}	4.04×10^{-9}	3.08×10^{-8}
Mean Data	0.38	5.18×10^3	0.50	4.42×10^{-7}	5.13×10^{-10}	3.02×10^{-8}
C1	0.77	3.69×10^3	0.13	0.22	1.05×10^{-11}	7.75×10^{-8}
C2	0.77	3.63×10^3	0.18	0.22	7.41×10^{-10}	7.50×10^{-8}
C3	0.41	1.92×10^3	0.18	0.28	6.25×10^{-10}	9.88×10^{-8}
C4	0.68	4.27×10^3	0.14	0.23	5.09×10^{-10}	1.66×10^{-7}
C5	0.78	4.11×10^3	0.16	0.26	4.14×10^{-11}	6.49×10^{-8}
C6	0.74	3.47×10^3	0.14	0.24	8.61×10^{-11}	8.63×10^{-8}
Mean	0.69	3.51×10^3	0.16	0.24	3.36×10^{-10}	9.48×10^{-8}
Median	0.75	3.66×10^3	0.15	0.23	2.98×10^{-10}	8.19×10^{-8}
SD	0.14	8.38×10^2	0.02	0.02	3.26×10^{-10}	3.67×10^{-8}
Mean Data	0.78	3.69×10^3	0.16	0.24	1.10×10^{-10}	8.42×10^{-8}
p-value	0.013	0.70	0.0049	0.005	0.24	0.94

doi:10.1371/journal.pcbi.1005127.t002

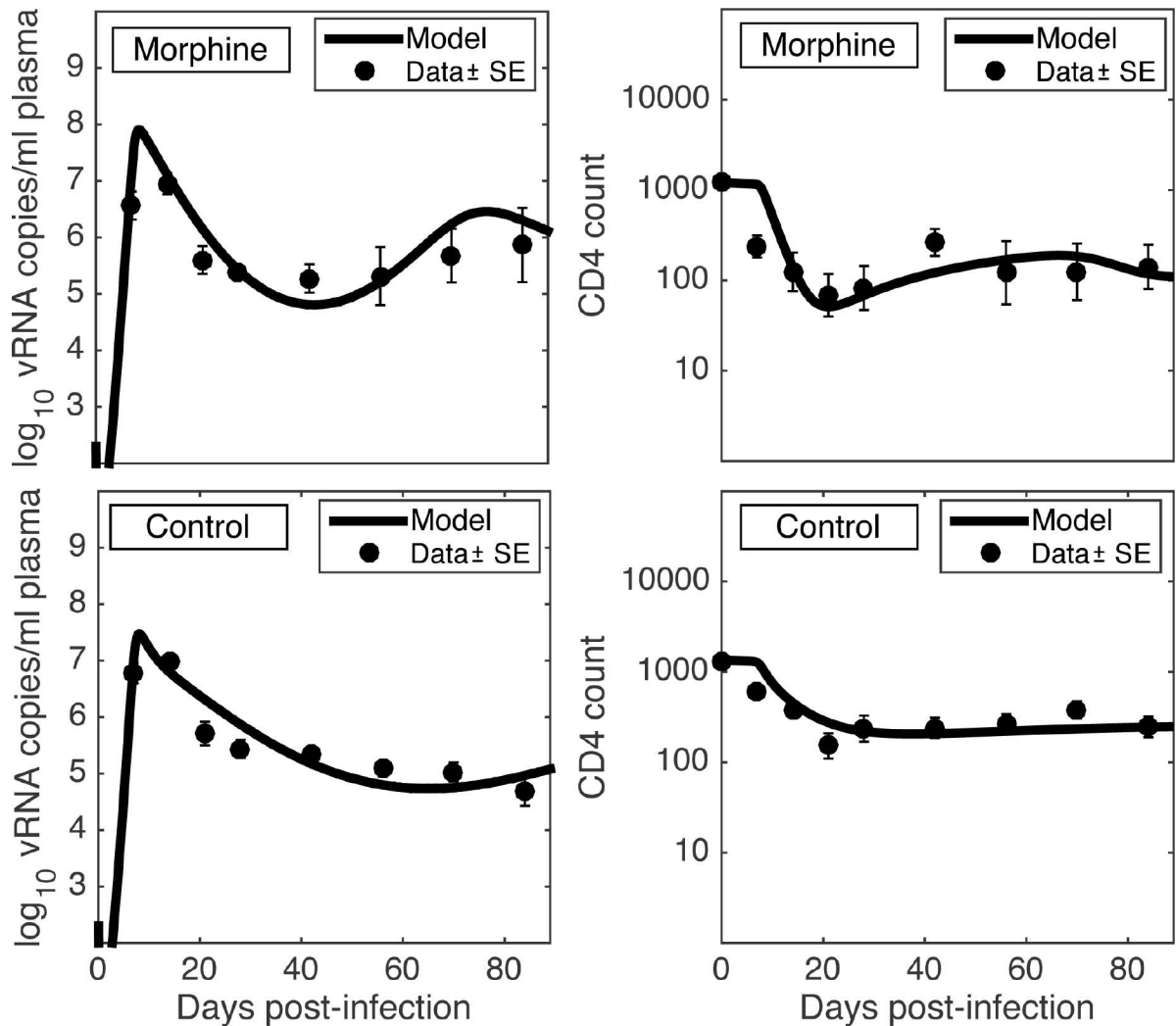


Fig 2. Model fit to the data. Best-fit viral load (left column) and CD4 count/microliter (right column) dynamics predicted by the model (solid line) along with the mean \log_{10} viral load and the mean CD4 count data (filled small circles with bars representing standard errors) for the morphine group (first row) and the control group (second row). Parameters used, including the best estimates for model parameters, are given in Table 2.

doi:10.1371/journal.pcbi.1005127.g002

infection rates β_l and β_h , corresponding to the infection of T_l and T_h cells, respectively (Table 2). We found that β_h is significantly higher than β_l (1 to 2 orders of magnitude higher in both the morphine and control groups), showing that T_h target cells are more susceptible to SIV infection than T_l target cells. This difference between β_l and β_h is statistically significant in the morphine group (t-test, $p < 0.001$), the control group (t-test, $p < 0.001$), as well as all animals combined (t-test, $p < 0.001$). The infection rate increase estimated here is in agreement with an experiment in which an increase in cells expressing CCR5 from 1.75% to 12.5% increased the p24 level by 2 orders of magnitude [44]. Note that the differences in β_l between the two groups and β_h between the two groups are not statistically significant (t-test, $p > 0.05$ for both tests, Table 2). This shows that there is a minimal contribution of variation in susceptibility among animals to the difference in infection susceptibility between two groups of target cells.

Effects of Morphine on Target Cell Subpopulation Switch

In our model, the rate of target cell subpopulation switch is represented by two parameters: r , the transfer rate from the T_l compartment to the T_h compartment, and q , the transfer rate from the T_h compartment to the T_l compartment. Our estimates indicate that morphine causes target cells to transfer from the T_l compartment to the T_h compartment about 3 times faster compared to the control environment [$r = 0.52 \pm 0.02$ per day in the morphine group vs. $r = 0.16 \pm 0.01$ per day in the control group]. The difference in r between two groups is statistically significant (t-test, $p < 0.005$). More importantly, the backward transfer rate, q , is significantly lower (t-test, $p = 0.005$) in the morphine group compared to the control group [$q = 1.02 \pm 0.75 \times 10^{-6}$ per day in the morphine group vs. $q = 0.24 \pm 0.01$ per day in the control group]. These parameter estimates strongly suggest that morphine can have an important role in altering the nature of target cells. The results are also in agreement with previous *in vitro* [27, 41] and *in vivo* [60] experiments that show morphine promotes co-receptor expression in target cells thereby increasing their susceptibility to HIV/SIV infection.

Basic Reproduction Number

The basic reproduction number, denoted by R_0 , is an important measure of host viral dynamics, as it determines whether a virus can establish infection [21, 61, 62]. R_0 is defined as the average number of cells infected by a single infected cell when there is no target cell limitation. In general, if $R_0 < 1$ the infection will die out, and if $R_0 > 1$ the infection will spread [21, 61, 62]. Using the next-generation method (see S1 Text), we derive the basic reproduction number of our model as:

$$R_0 = \frac{\lambda p}{\delta c d (d + r + q)} [\beta_l (d + q) + \beta_h r] \quad (5)$$

Substituting our parameter estimates into Eq (5), we obtained $R_0 = 2.08$ for the control group and $R_0 = 9.69$ for the morphine group. With $R_0 > 1$ in both groups, our model predicts that the infection spreads in both groups, consistent with the data. Moreover, these estimates show that the morphine can significantly affect the basic reproduction number.

Long-Term Effects of Morphine

In the absence of SIV infection. In the absence of SIV infection, i.e. $V = I = 0$, the model reduces to

$$\frac{dT_l}{dt} = \lambda + qT_h - dT_l - rT_l, \quad T_l(0) = T_{l0}, \quad (6)$$

$$\frac{dT_h}{dt} = rT_l - dT_h - qT_h, \quad T_h(0) = T_{h0}, \quad (7)$$

Further, in the absence of infection, the total T cells in circulation remains approximately constant, i.e. $\frac{d(T_l + T_h)}{dt} = 0$, giving $\lambda = d(T_l + T_h)$. In this case, the proportion of T_h cells, $x = T_h / (T_l + T_h)$, is given by the solution of

$$\frac{dx}{dt} = r - (d + r + q)x \quad (8)$$

Solving Eq (8), we obtain the time-dependent solution for the proportion of T_h cells as

$$x(t) = \frac{r}{(d+r+q)} + \left[x(0) - \frac{r}{(d+r+q)} \right] e^{-(d+r+q)t} \quad (9)$$

Taking the limit as $t \rightarrow \infty$ in Eq (9), we obtain that in long-term morphine conditioning, the proportion of T_h cells reaches $r/(d+r+q)$ in the absence of infection.

In the presence of SIV infection. To understand the effects of morphine on the long-term dynamics during SIV infection, we analyze two possible steady states, the infection-free steady state, E^0 , and the infected steady state, E^* . The infection free steady state, is given by

$$E^0 = (T_l^0, T_h^0, I^0, V^0) = \left(\frac{\lambda(d+q)}{d(d+r+q)}, \frac{\lambda r}{d(d+r+q)}, 0, 0 \right).$$

Linearizing the system around E^0 , and analyzing the eigenvalues of the Jacobian matrix, we can prove that E^0 is asymptotically stable if $R_0 < 1$ and unstable if $R_0 > 1$ (see S1 Text) as discussed above.

For the analysis of the infected steady state during morphine conditioning, we assume $\beta_l \ll \beta_h$ and $q \ll r$, as given by our parameter estimates, in order to simplify the model. In this case, E^* is given by

$$E^* = (T_l^*, T_h^*, I^*, V^*) = \left(\frac{\lambda}{d+r}, \frac{\delta c}{\beta_h p}, \frac{dc}{\beta_h p} (R_0 - 1), \frac{d}{\beta_h} (R_0 - 1) \right).$$

Clearly, E^* exists if $R_0 > 1$. Furthermore, we are able to prove that E^* , if it exists, is asymptotically stable (see S1 Text). This expression shows that a higher value of R_0 as in morphine group gives a higher equilibrium viral load.

We then carried out simulations of the full model to analyze effects of morphine on the dynamics as well as the infected-steady state level. For about 5–6 weeks post-infection, the plasma viral load dynamics remained generally comparable in both the morphine and control groups. However, after 6 weeks of infection the viral load in the morphine group increases and eventually approaches a higher steady state level (Fig 3). In contrast to the morphine group, the viral load in the control group did not increase and leveled off with about a 1.0 \log_{10} lower steady state value. We also observed how the percentage of target cells in T_h compartment changes over time (Fig 3). In both groups, the percentage of target cells in the T_h compartment decreases after infection following a brief delay, reaches a minimum, and again increases to a steady state level. Throughout the dynamics, this percentage in the morphine group almost always remained higher than in the control group, with a significantly higher steady state level in the morphine group (Fig 3).

Since morphine conditioning results in a higher steady state level of target cells in the T_h compartment, which have a higher infection rate, morphine was expected to cause a greater loss of CD4 cells. To quantify this, we simulated the dynamics of CD4 cells (Fig 4) and computed the total loss of CD4 cells during one year of SIV infection. Our model predicts a rapid decrease of the CD4 count in the morphine group compared to the control group at the beginning of the infection, consistent with the experimental data. At the end of a year, the predicted total CD4 count drop is 90% in the morphine group while it is 82% in the control group (Fig 4). The difference in CD4 loss between the two groups is not statistically significant (t-test, $p > 0.05$). However, animal M4 has an extremely high CD4 count throughout the infection (see Table 1, S1 Fig); and its set point CD4 count remains higher than 700 cells/ μ L while the maximum set point CD4 count of all other animals in the morphine group is 42 cells/ μ L.

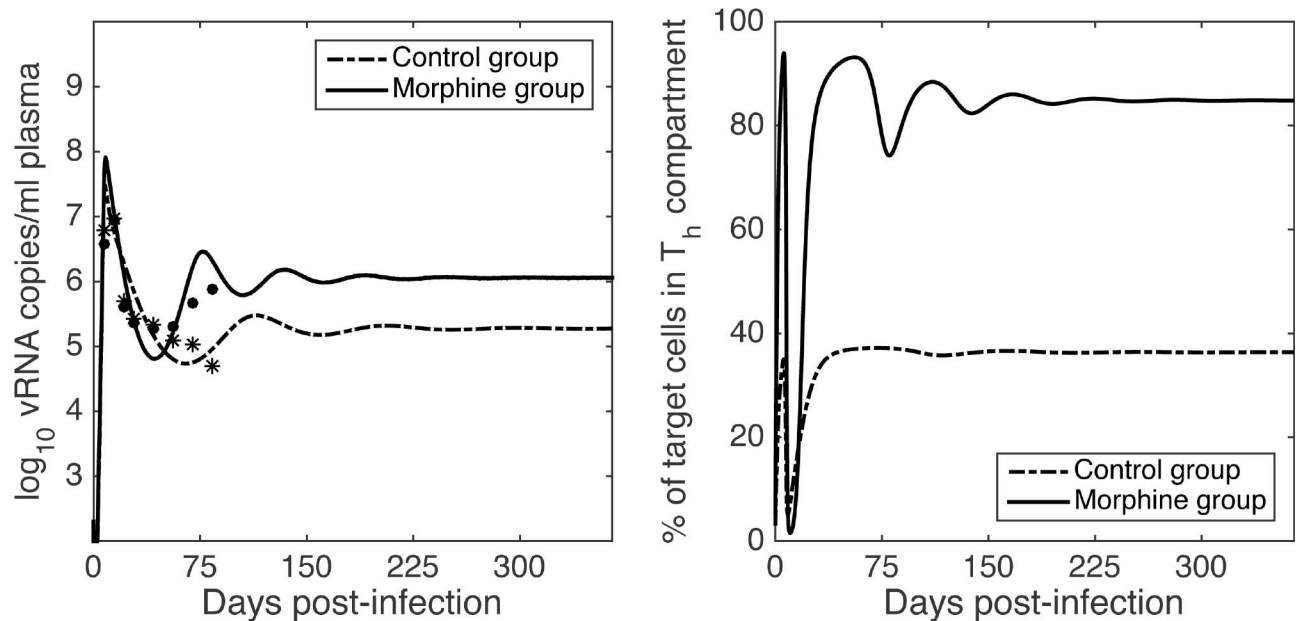


Fig 3. Long term dynamics of viral load and T cell subpopulations. Long term dynamics, predicted by the model, of the viral load (left) and the % of target cells that are T_h cells (right) for the morphine group (dashed-dot curve) and the control group (solid curve). Parameters given in Table 2 are used for model simulations. Small circles indicate the available data, which is restricted to time points early in infection.

doi:10.1371/journal.pcbi.1005127.g003

Excluding animal M4, the loss of CD4 cells in the morphine group is significantly higher than that in the control group (t-test, $p < 0.001$).

Effect of Morphine in the Presence of Antiretroviral Therapy

While morphine does not seem to play a role in determining whether infection is established or not as $R_0 > 1$ in both groups, a significantly higher R_0 value in the morphine group comes

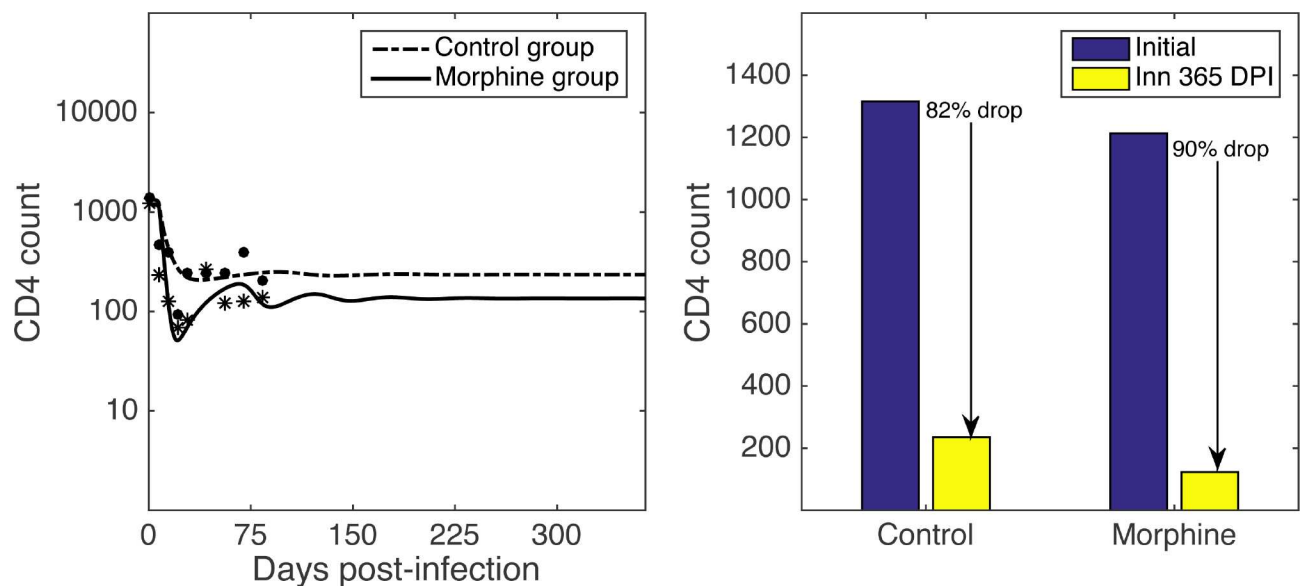


Fig 4. CD4 count dynamics. Model prediction for the long term dynamics of CD4 count (left) and the total loss of CD4 count during a year of SIV infection (right) for the morphine group (dashed-dot curve) and the control group (solid curve). Parameters given in Table 2 are used for model simulations. Small circles indicate the available data.

doi:10.1371/journal.pcbi.1005127.g004

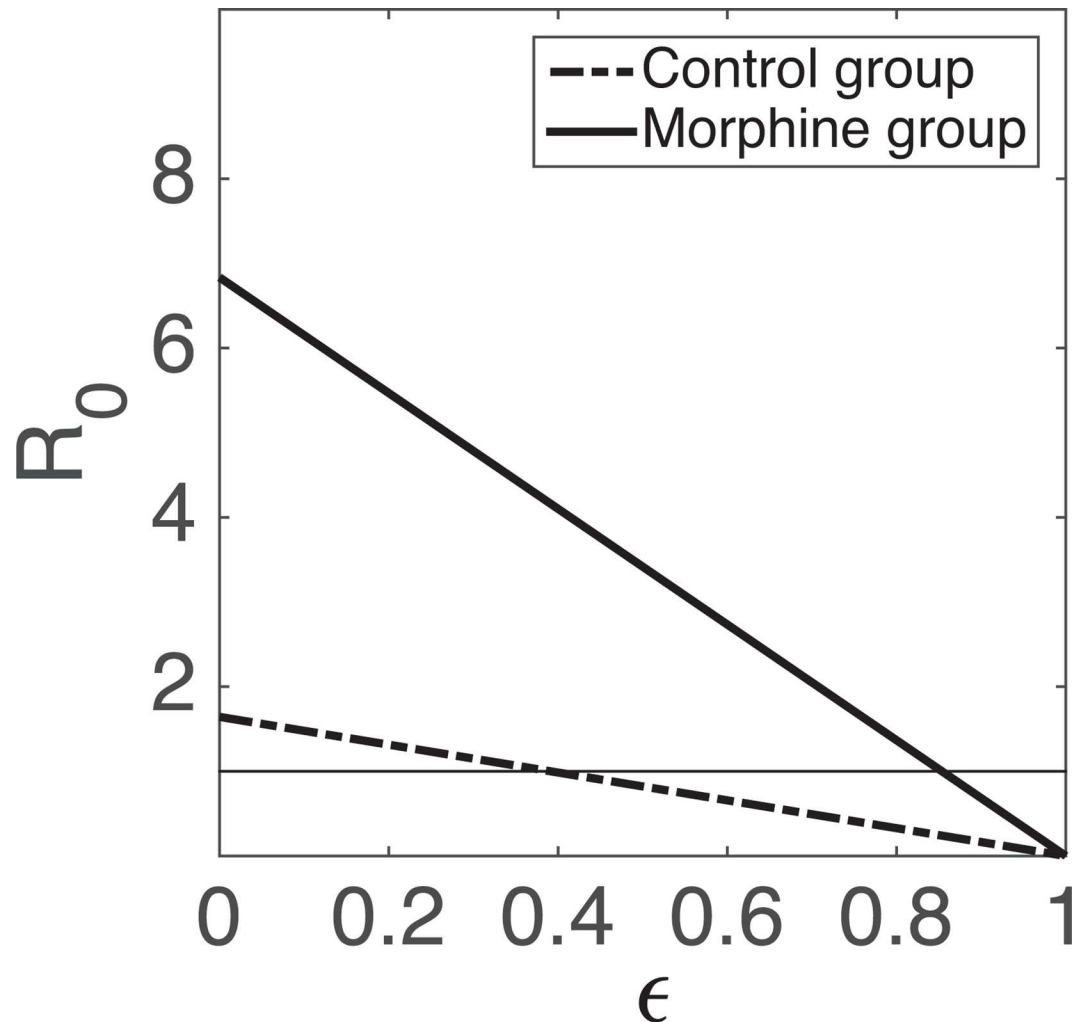


Fig 5. Dependence of the value of R_0 on ϵ , efficacy of ART. Parameters given in Table 2 are used for computation of R_0 . The dashed-dot line represents the control group while the solid line represents the morphine group.

doi:10.1371/journal.pcbi.1005127.g005

into play when some interventions, such as antiretroviral therapy as pre-exposure prophylaxis (PrEP), are considered. If ϵ is the efficacy of PrEP, then $\epsilon > 1 - 1/R_0$ is needed for successful control of infection (i.e., for bringing the R_0 value to less than 1). Thus, we estimate that at least 52% effective PrEP can control infection in the control group, while at least 90% efficacy of PrEP is required in the morphine group. Fig 5 shows how R_0 depends on PrEP efficacy. These results suggest that morphine can decrease the effectiveness of PrEP in people who abuse drugs.

Significant effects of morphine can also be seen in post infection antiretroviral therapy (ART) as demonstrated by model simulations with early ART initiation (14 days post infection) and late ART initiation (200 days post infection) (Fig 6). Whether ART can control viral load or not depends upon the efficacy of ART. While the high ART efficacy, $\epsilon = 0.95$, can successfully control the virus in both groups, the viral suppression is more effective in the control group than in the morphine group in general (Fig 6). Most importantly, for intermediate level of ART efficacy (for example, 60% in our simulation), ART can suppress the viral load in the

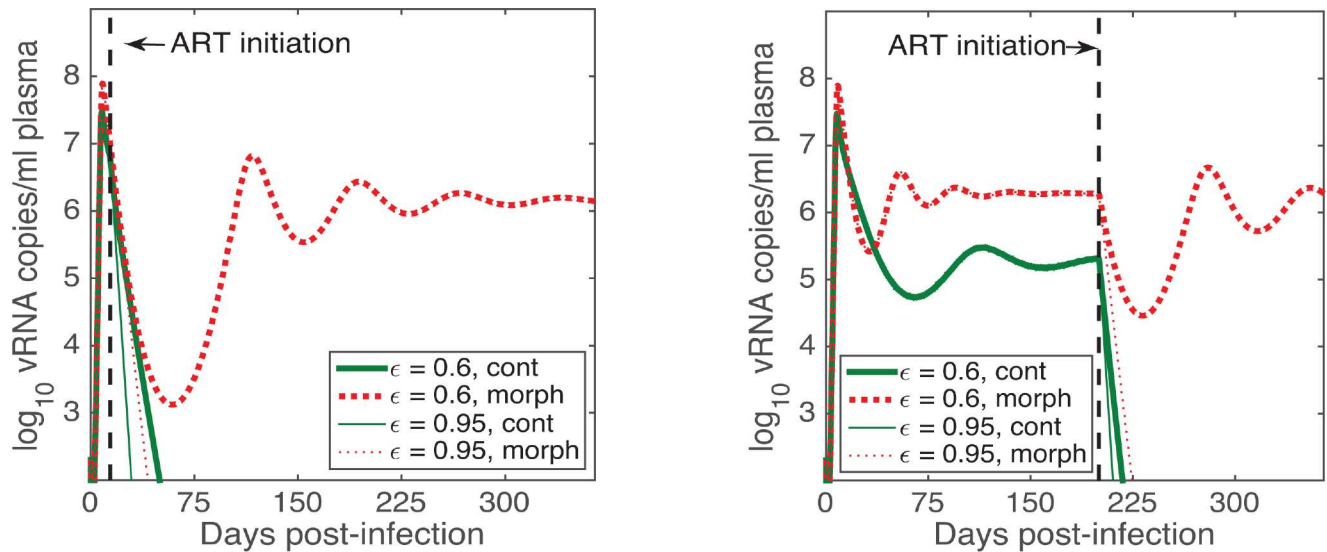


Fig 6. Predicted effects of morphine on antiretroviral therapy. Early ART is initiated 14 days post infection (left) and late ART is initiated 200 days post infection (right). The solid lines represent the control group and the dotted lines represent the morphine group. Two different ART efficacies, 0.6 (medium), and 0.95 (high), are simulated. Parameters given in Table 2 are used for model simulations.

doi:10.1371/journal.pcbi.1005127.g006

control group, but fails to suppress in the morphine group with both early and late ART initiation (Fig 6). Note that the value of $\epsilon = 0.95$ and 0.6 are taken only for demonstration purposes. While current combination ARTs are highly efficacious, it is possible to have lower efficacies due to lack of compliance or emergence of resistance. Further, some combination therapies have been estimated to have efficacies in the 60 to 70% range [63].

Sensitivity to V_0 and T_{h0}

Due to lack of information about the actual number of virions that initiate infection, we studied how our parameter estimates are affected by the choice of V_0 . We considered 500 different values of V_0 selected randomly from 1 to 4 \log_{10} viral RNA copies/ml. For each V_0 selected, we estimated parameters for the morphine group as well as the control group. The box and whisker plots of the parameter estimates (S2 Fig) showed that the median change of each estimate remains less than 10% of the base case estimate. Also, based on *in vitro* experiments [41] we chose the initial proportion of T_h cells as 5% (morphine) and 3% (control) of the total target cell. Varying this value from 1 to 15% did not make any significant change in our estimates (less than 5% in each parameter estimate). Thus, our estimates are robust within these ranges of V_0 and T_{h0} .

Discussion

The dependence of many HIV-infected patients on drugs of abuse such as opiates is an ongoing problem in the post-HAART era. Although injection drug use is one of the important risk factors for HIV infection, with IDU constituting approximately one-third of new AIDS cases in the USA, the relationship between IDU and HIV-1 dynamics remains unclear. In this study, we developed a novel morphine-conditioned viral dynamics model, which is in agreement with experimental data on viral loads and CD4+ T-cell counts in SIV/SHIV infected rhesus macaques (Fig 2 and S1 Fig). This study provides for the first time estimates of SIV viral

dynamic parameters in the presence of a drug of abuse. Our model offers insight into how morphine can affect SIV infection and progression.

Our model and parameter estimates support the experimental observation [26, 27, 41, 45, 46] that morphine promotes co-receptor expression in target cells (CD4⁺ T cells), thereby increasing the susceptibility of these cells to HIV/SIV infection. For SIV/SHIV infected rhesus macaques, we estimated the levels of two target cell subpopulations: one group (T_h) with an infection rate about 2 orders of magnitude higher than the other group (T_l) ($p < 0.001$). Moreover, our estimates show that the rate of switch between these two subpopulations is greatly affected by morphine ($p < 0.005$) that causes a three-fold higher rate of transfer from T_l to T_h cells with almost negligible flow of cells in other direction (Table 2). While the precise mechanism by which morphine alters co-receptor expression remains to be determined, the finding of morphine promoting co-receptor expression can be related to the well-established capacity of opioids to alter cytokine release [27, 41, 64]. Morphine may activate the release of cytokines (e.g. tumor necrosis factor- α or IL-2) known to stimulate chemokine receptor expression or morphine may inhibit the synthesis of certain chemokines (e.g., RANTES) that cause internalization of co-receptors.

A morphine effect on increasing co-receptor expression is consistent with *in vitro* and *in vivo* experiments [27, 41, 60] as well as the results here on the increased transition from T_l to T_h cells in the morphine-dependent group. Furthermore, based on simulation results in the presence of infection, in the long run, the percentage of T_h target cells in the morphine group can reach an extremely high level (almost 85%, Fig 3). These predicted levels are higher than seen in previous experiments [60] and suggests that either morphine exposure in the absence of SIV infection might not have been long enough to reach the steady state in the experimental studies [27, 41, 60] or the rate of subpopulation switch is different in the presence of SIV infection. If the latter is true, it indicates that not only does morphine alter viral infection, but also viral infection alters the effects of morphine. Further experiments, particularly, on long-term morphine effects in the absence of HIV/SIV infection will be necessary to clarify this issue.

Our estimates show that R_0 is higher in morphine-dependent animals than in control animals, indicating that morphine may induce additional obstacles for intervention strategies such as ART as PrEP. For example, a higher efficacy of ART used for PrEP may be required for morphine-dependent populations than for the general population. We note that the R_0 values estimated for morphine-dependent animals (9.69) and control animals (2.08), although low, both fall within the approximate range of previously estimated R_0 values for HIV/SIV [29, 65]. Therefore, we cannot be definite on whether the elevated R_0 value in the morphine group is due to the presence of morphine or some other causes such as variation among hosts. Further analysis with larger data sets is needed to better understand the effects of morphine on R_0 .

Using steady state analysis and model simulations, we studied the long-term dynamics. Since $R_0 > 1$ in both the morphine and control groups, the infection free steady state is unstable and infection was established in these animals as reported earlier [16]. A marked difference was seen in the steady state viral load levels in these two groups; with the viral load steady state being 1.0 \log_{10} higher in the morphine group than in the control group (Fig 3). The dynamics predicted by the model also shows that the total CD4⁺ T-cell count decreases faster in the morphine group than in the control group, particularly during the acute phase of infection. The model predicts that there is a higher CD4⁺ T-cell count drop in the morphine group than in the control group (90% drop in morphine group vs. 82% drop in control group after a year of SIV infection, Fig 4). This drop is not statistically significant when all animals are included in the analysis, but it becomes significant when animal M4 with an unusually high CD4⁺ T-cell count is excluded from the analysis. While we need more data to accurately evaluate the significance of the predicted CD4⁺ T-cell count drop, the current results suggest that the morphine

may exacerbate the progression and pathogenesis of HIV/SIV infection in agreement with the experimental observations.

Effect of morphine is also clearly revealed in our model simulations in the presence of ART (Fig 6); morphine conditioning makes it harder to control the viral load with both early and late ART initiations. Most notably, for an intermediate level of drug efficacy, ART may fail to control the viral load in morphine-dependent individuals but control the viral load in non-dependent individuals. This suggests that to achieve treatment success, the ART protocol for patients with a drug addiction may have to be different than for patients without drug addictions.

We acknowledge several limitations of this study. Our parameter estimates are based on a limited data set. A larger data set obtained in both the presence and absence of HIV/SIV infection would help us gain more confidence in the estimated parameter values and related results. Our model also does not distinguish between the two main HIV/SIV co-receptors, CCR5 and CXCR4. While morphine increases cell surface levels of both of these co-receptors [41], the level of expression induced by morphine may be different between the two; one study [60] indicates that the effect of morphine on CCR5 expression is more pronounced compared to CXCR4 expression. Since 2 of the 3 viruses used in this experiment are either dual-tropic or R5-tropic, our results may be more applicable to CCR5 viruses. Our results may need to be considered carefully in the case of X4 viruses if CXCR4 expression responds differently to morphine exposure.

Our model is focused on the effect of morphine on inducing co-receptor expression. Other physiological alterations induced by morphine could also have an impact on viral kinetics. For example, morphine could lead to differences in inflammation status, or in the viral dynamics across the blood-brain barrier, or in immune responses. Here we did not try to study exhaustively all these other factors. We did however analyze the potential for immune effects to explain the differences between the observed viral dynamics in the presence and absence of morphine (see S2 Text). We fitted two immune response models, including cytolytic or non-cytolytic effects, but found that these provided much poorer fits to the data than our model based on differences in target cell susceptibility. Indeed, using AICc, we showed that the data provide much better support for the latter model. While these basic models (as well as the experimental results discussed above) do not support noticeable effects of morphine on immune responses, a more detailed analysis using models including immune responses [34–37] and tissue compartments can be developed, but would involve additional parameters and require more data to validate. In this context, it is interesting that we found a statistically significant lower δ , the death rate of productively infected cells, in the morphine group ($p < 0.05$). This seems to indicate that a less vigorous immune response may also be a result of morphine, although it is not sufficient to explain the difference in viral dynamics based on our analyses of the immune response models. Thus, quantifying other effects of morphine on the immune system and on viral dynamics via modeling will continue to be an active field of investigation. For example, we suggest that an experiment in which ART is given to morphine-conditioned vs. control animals may provide a better indication for differences in the death rate of productively infected cells.

Supporting Information

S1 Text. Mathematical analysis of the model.

(PDF)

S2 Text. Analyses of immune response models with cytolytic or non-cytolytic effects.

(PDF)

S1 Table. 95% Confidence intervals for the estimated model parameters.
(PDF)

S1 Fig. Model fit to the data from individual monkeys.
(PDF)

S2 Fig. Sensitivity of the fitted model parameters to the initial viral load V_0 .
(PDF)

Author Contributions

Conceptualization: NKV AK.

Formal analysis: NKV RMR ASP.

Funding acquisition: NKV.

Investigation: AK.

Methodology: NKV.

Project administration: NKV.

Software: NKV RMR.

Supervision: NKV.

Writing – original draft: NKV.

Writing – review & editing: NKV RMR ASP AK.

References

1. Beyrer C, Razak MH, Lisam K, Chen J, Lui W, Yu XF. Overland heroin trafficking routes and HIV-1 spread in south and south-east Asia. *Aids*. 2000; 14(1):75–83. Epub 2000/03/14. PMID: [10714570](#).
2. Francis H. Substance abuse and HIV infection. *Topics in HIV Med*. 2003; 11(1):20–4. Epub 2003/04/30. PMID: [12717047](#).
3. Reddy PV, Pilakka-Kanthikeel S, Saxena SK, Saiyed Z, Nair MP. Interactive effects of morphine on HIV infection: Role in HIV-associated neurocognitive disorder. *AIDS Research and Treatment*. 2012; 2012:953678. Epub 2012/06/06. doi: [10.1155/2012/953678](#) PMID: [22666564](#); PubMed Central PMCID: PMC3362817.
4. CDC. Drug-associated HIV transmission continues in the United States. 2007; April 12, 2013.
5. Antinori A, Arendt G, Becker JT, Brew BJ, Byrd DA, Cherner M, et al. Updated research nosology for HIV-associated neurocognitive disorders. *Neurology*. 2007; 69(18):1789–99. Epub 2007/10/05. doi: [10.1212/01.WNL.0000287431.88658.8b](#) PMID: [17914061](#).
6. Bell JE, Anthony IC, Simmonds P. Impact of HIV on regional & cellular organisation of the brain. *Current HIV Res*. 2006; 4(3):249–57. Epub 2006/07/18. PMID: [16842078](#).
7. Bell JE, Brettle RP, Chiswick A, Simmonds P. HIV encephalitis, proviral load and dementia in drug users and homosexuals with AIDS. Effect of neocortical involvement. *Brain: a journal of neurology*. 1998; 121 (Pt 11):2043–52. Epub 1998/11/25. PMID: [9827765](#).
8. Nath A, Maragos WF, Avison MJ, Schmitt FA, Berger JR. Acceleration of HIV dementia with methamphetamine and cocaine. *J Neurovirology*. 2001; 7(1):66–71. Epub 2001/08/25. doi: [10.1080/135502801300069737](#) PMID: [11519485](#).
9. Donahoe RM, O'Neil S P, Marsteller FA, Novembre FJ, Anderson DC, Lankford-Turner P, et al. Probable deceleration of progression of Simian AIDS affected by opiate dependency: studies with a rhesus macaque/SIVsmm9 model. *JAIDS* 2009; 50(3):241–9. Epub 2009/02/06. doi: [10.1097/QAI.0b013e3181967354](#) PMID: [19194320](#).
10. Alcapes P, Friedland G. Injection drug use and human immunodeficiency virus infection. *Clinical Infect Dis* 1995; 20(6):1467–79. Epub 1995/06/01. PMID: [7548494](#).

11. Donahoe RM. Neuroimmunomodulation by opiates: relationship to HIV-1 infection and AIDS. *Adv Neuroimmunol.* 1993; 3:3146.
12. Donahoe RM, Vlahov D. Opiates as potential cofactors in progression of HIV-1 infections to AIDS. *J Neuroimmunol.* 1998; 83(1–2):77–87. Epub 1998/06/04. PMID: [9610676](#).
13. Kapadia F, Vlahov D, Donahoe RM, Friedland G. The role of substance abuse in HIV disease progression: reconciling differences from laboratory and epidemiologic investigations. *Clinical Infect Dis: an official publication of the Infectious Diseases Society of America.* 2005; 41(7):1027–34. Epub 2005/09/06. doi: [10.1086/433175](#) PMID: [16142670](#).
14. Selwyn PA, Alcabes P, Hartel D, Buono D, Schoenbaum EE, Klein RS, et al. Clinical manifestations and predictors of disease progression in drug users with human immunodeficiency virus infection. *N Eng J Med.* 1992; 327(24):1697–703. Epub 1992/12/10. doi: [10.1056/NEJM199212103272401](#) PMID: [1359411](#).
15. Kumar R, Orsoni S, Norman L, Verma AS, Tirado G, Giavedoni LD, et al. Chronic morphine exposure causes pronounced virus replication in cerebral compartment and accelerated onset of AIDS in SIV/SHIV-infected Indian rhesus macaques. *Virology.* 2006; 354(1):192–206. Epub 2006/08/01. doi: [10.1016/j.virol.2006.06.020](#) PMID: [16876224](#).
16. Kumar R, Torres C, Yamamura Y, Rodriguez I, Martinez M, Staprans S, et al. Modulation by morphine of viral set point in rhesus macaques infected with simian immunodeficiency virus and simian-human immunodeficiency virus. *J Virol.* 2004; 78(20):11425–8. doi: [10.1128/JVI.78.20.11425-11428.2004](#) PMID: [15452267](#); PubMed Central PMCID: [PMC4095870](#).
17. Rivera-Amill V, Silverstein PS, Noel RJ Jr., Kumar S, Kumar A. Morphine and rapid disease progression in nonhuman primate model of AIDS: inverse correlation between disease progression and virus evolution. *J Neuroimmune Pharmacology: the official journal of the Society on NeuroImmune Pharmacology.* 2010; 5(1):122–32. Epub 2009/12/17. doi: [10.1007/s11481-009-9184-0](#) PMID: [20013315](#); PubMed Central PMCID: [PMC4095870](#).
18. Rivera-Amill V, Kumar R, Noel RJ, Garcia Y, Rodriguez IV, Martinez M, et al. Short communication: Lack of immune response in rapid progressor morphine-dependent and SIV/SHIV-infected rhesus macaques is correlated with downregulation of TH1 cytokines. *AIDS Res Human Retroviruses.* 2010; 8:919–22.
19. Tirado G, Kumar A. Evolution of SIV envelope in morphine-dependent rhesus macaques with rapid disease progression. *AIDS research and human retroviruses.* 2006; 22(1):114–9. Epub 2006/01/28. doi: [10.1089/aid.2006.22.114](#) PMID: [16438654](#).
20. Wang Y, Wang X, Ye L, Li J, Song L, Fulambarkar N, et al. Morphine suppresses IFN signaling pathway and enhances AIDS virus infection. *PLoS One.* 2012; 7(2):e31167. Epub 2012/02/24. doi: [10.1371/journal.pone.0031167](#) PMID: [22359571](#); PubMed Central PMCID: [PMC3281044](#).
21. Bonhoeffer S, May RM, Shaw GM, Nowak MA. Virus dynamics and drug therapy. *Proc Natl Acad Sci USA* 1997; 94(13):6971–6. Epub 1997/06/24. PMID: [9192676](#); PubMed Central PMCID: [PMC21269](#).
22. Nowak MA, May RM. *Virus dynamics: mathematical principles of immunology and virology.* New York: Oxford University Press; 2000.
23. Perelson AS. Modelling viral and immune system dynamics. *Nature reviews Immunology.* 2002; 2(1):28–36. Epub 2002/03/22. doi: [10.1038/nri700](#) PMID: [11905835](#).
24. Perelson AS, Ribeiro RM. Modeling the within-host dynamics of HIV infection. *BMC biology.* 2013; 11:96. doi: [10.1186/1741-7007-11-96](#) PMID: [24020860](#); PubMed Central PMCID: [PMC3765939](#).
25. Guo CJ, Li Y, Tian S, Wang X, Douglas SD, Ho WZ. Morphine enhances HIV infection of human blood mononuclear phagocytes through modulation of beta-chemokines and CCR5 receptor. *J Investig Med.* 2002; 50(6):435–42. PMID: [12425430](#); PubMed Central PMCID: [PMC4037869](#). doi: [10.1136/jim-50-06-03](#)
26. Li Y, Merrill JD, Mooney K, Song L, Wang X, Guo CJ, et al. Morphine enhances HIV infection of neonatal macrophages. *Pediatr Res.* 2003; 54(2):282–8. doi: [10.1203/01.PDR.0000074973.83826.4C](#) PMID: [12736382](#); PubMed Central PMCID: [PMC4035124](#).
27. Suzuki S, Chuang AJ, Chuang LF, Doi RH, Chuang RY. Morphine promotes simian acquired immunodeficiency syndrome virus replication in monkey peripheral mononuclear cells: induction of CC chemokine receptor 5 expression for virus entry. *J Infect Dis.* 2002; 185(12):1826–9. doi: [10.1086/340816](#) PMID: [12085334](#).
28. Little SJ, McLean AR, Spina CA, Richman DD, Havlir DV. Viral dynamics of acute HIV-1 infection. *The Journal of experimental medicine.* 1999; 190(6):841–50. Epub 1999/09/28. PMID: [10499922](#); PubMed Central PMCID: [PMC2195636](#).
29. Nowak MA, Lloyd AL, Vasquez GM, Wiltout TA, Wahl LM, Bischofberger N, et al. Viral dynamics of primary viremia and antiretroviral therapy in simian immunodeficiency virus infection. *J Virol.* 1997; 71(10):7518–25. Epub 1997/10/06. PMID: [9311831](#); PubMed Central PMCID: [PMC192098](#).

30. Perelson AS, Nelson PW. Mathematical analysis of HIV-1 dynamics of vivo. *SIAM Rev.* 1999; 41:344.
31. Phillips AN. Reduction of HIV concentration during acute infection: independence from a specific immune response. *Science.* 1996; 271(5248):497–9. Epub 1996/01/26. PMID: [8560262](#).
32. Stafford MA, Corey L, Cao Y, Daar ES, Ho DD, Perelson AS. Modeling plasma virus concentration during primary HIV infection. *J Theor Biol.* 2000; 203(3):285–301. doi: [10.1006/jtbi.2000.1076](#) PMID: [10716909](#).
33. Vaidya NK, Ribeiro RM, Miller CJ, Perelson AS. Viral dynamics during primary simian immunodeficiency virus infection: effect of time-dependent virus infectivity. *J Virol.* 2010; 84(9):4302–10. doi: [10.1128/JVI.02284-09](#) PMID: [20147390](#); PubMed Central PMCID: [PMC2863724](#).
34. Schmitz JE, Kuroda MJ, Santra S, Sasseville VG, Simon MA, Lifton MA, et al. Control of viremia in simian immunodeficiency virus infection by CD8+ lymphocytes. *Science.* 1999; 283(5403):857–60. PMID: [9933172](#).
35. Burg D, Rong L, Neumann AU, Dahari H. Mathematical modeling of viral kinetics under immune control during primary HIV-1 infection. *J Theor Biol.* 2009; 259(4):751–9. doi: [10.1016/j.jtbi.2009.04.010](#) PMID: [19389409](#).
36. Regoes RR, Antia R, Garber DA, Silvestri G, Feinberg MB, Staprans SI. Roles of target cells and virus-specific cellular immunity in primary simian immunodeficiency virus infection. *Journal of virology.* 2004; 78(9):4866–75. PMID: [15078967](#); PubMed Central PMCID: [PMC2863724](#).
37. Tomaras GD, Yates NL, Liu P, Qin L, Fouda GG, Chavez LL, et al. Initial B-cell responses to transmitted human immunodeficiency virus type 1: virion-binding immunoglobulin M (IgM) and IgG antibodies followed by plasma anti-gp41 antibodies with ineffective control of initial viremia. *J Virol.* 2008; 82(24):12449–63. doi: [10.1128/JVI.01708-08](#) PMID: [18842730](#); PubMed Central PMCID: [PMC2593361](#).
38. Bar KJ, Tsao CY, Iyer SS, Decker JM, Yang Y, Bonsignori M, et al. Early low-titer neutralizing antibodies impede HIV-1 replication and select for virus escape. *PLoS Pathog.* 2012; 8(5):e1002721. doi: [10.1371/journal.ppat.1002721](#) PMID: [22693447](#); PubMed Central PMCID: [PMC3364956](#).
39. Elemans M, Seich AI, Basatena NK, Klatt NR, Gkekas C, Silvestri G, Asquith B. Why don't CD8+ T cells reduce the lifespan of SIV-infected cells in vivo? *PLoS Comput Biol.* 2011; 7(9):e1002200. doi: [10.1371/journal.pcbi.1002200](#) PMID: [21990968](#); PubMed Central PMCID: [PMC3182865](#).
40. Kouyos RD, Gordon SN, Staprans SI, Silvestri G, Regoes RR. Similar impact of CD8+ T cell responses on early virus dynamics during SIV infections of rhesus macaques and sooty mangabeys. *PLoS Comput Biol.* 2010; 6(8). doi: [10.1371/journal.pcbi.1000901](#) PMID: [20865048](#); PubMed Central PMCID: [PMC2928736](#).
41. Steele AD, Henderson EE, Rogers TJ. Mu-opioid modulation of HIV-1 coreceptor expression and HIV-1 replication. *Virology.* 2003; 309(1):99–107. PMID: [12726730](#).
42. Lehner T. The role of CCR5 chemokine ligands and antibodies to CCR5 coreceptors in preventing HIV infection. *Trends in immunology.* 2002; 23(7):347–51. Epub 2002/07/10. PMID: [12103354](#).
43. Stantchev TS, Broder CC. Human immunodeficiency virus type-1 and chemokines: beyond competition for common cellular receptors. *Cytokine & growth factor reviews.* 2001; 12(2–3):219–43. Epub 2001/04/28. PMID: [11325604](#).
44. Wu L, Paxton WA, Kassam N, Ruffing N, Rottman JB, Sullivan N, et al. CCR5 levels and expression pattern correlate with infectability by macrophage-tropic HIV-1, in vitro. *J Exp Med.* 1997; 185(9):1681–91. PMID: [9151905](#); PubMed Central PMCID: [PMC2196298](#).
45. Bokhari SM, Yao H, Bethel-Brown C, Fuwang P, Williams R, Dhillion NK, et al. Morphine enhances Tat-induced activation in murine microglia. *J Neurovirology.* 2009; 15(3):219–28. Epub 2009/05/23. doi: [10.1080/13550280902913628](#) PMID: [19462331](#); PubMed Central PMCID: [PMC3121575](#).
46. Mahajan SD, Schwartz SA, Aalinkeel R, Chawda RP, Sykes DE, Nair MP. Morphine modulates chemokine gene regulation in normal human astrocytes. *Clinical Immunology.* 2005; 115(3):323–32. Epub 2005/05/17. doi: [10.1016/j.cim.2005.02.004](#) PMID: [15893700](#).
47. Burnham KP, Anderson DR. *Model Selection and Multimodel Inference: A Practical Information-Theoretic Approach.* 2nd edition ed. New York: Springer; 2002.
48. Ramratnam B, Bonhoeffer S, Binley J, Hurley A, Zhang L, Mittler JE, et al. Rapid production and clearance of HIV-1 and hepatitis C virus assessed by large volume plasma apheresis. *Lancet.* 1999; 354(9192):1782–5. Epub 1999/11/30. doi: [10.1016/S0140-6736\(99\)02035-8](#) PMID: [10577640](#).
49. Zhang L, Dailey PJ, Gettie A, Blanchard J, Ho DD. The liver is a major organ for clearing simian immunodeficiency virus in rhesus monkeys. *J Virol.* 2002; 76(10):5271–3. Epub 2002/04/23. PMID: [11967341](#); PubMed Central PMCID: [PMC136155](#).

50. Sachsenberg N, Perelson AS, Yerly S, Schockmel GA, Leduc D, Hirschel B, et al. Turnover of CD4+ and CD8+ T lymphocytes in HIV-1 infection as measured by Ki-67 antigen. *J Exp Med.* 1998; 187(8):1295–303. Epub 1998/05/23. PMID: [9547340](#); PubMed Central PMCID: PMC2212238.
51. Chen HY, Di Mascio M, Perelson AS, Ho DD, Zhang L. Determination of virus burst size in vivo using a single-cycle SIV in rhesus macaques. *Proc Natl Acad Sci USA* 2007; 104(48):19079–84. Epub 2007/11/21. doi: [10.1073/pnas.0707449104](#) PMID: [18025463](#); PubMed Central PMCID: PMC2141911.
52. Markowitz M, Louie M, Hurley A, Sun E, Di Mascio M, Perelson AS, et al. A novel antiviral intervention results in more accurate assessment of human immunodeficiency virus type 1 replication dynamics and T-cell decay in vivo. *J Virol.* 2003; 77(8):5037–8. Epub 2003/03/29. PMID: [12663814](#); PubMed Central PMCID: PMC152136.
53. Ma ZM, Stone M, Piatak M Jr., Schweighardt B, Haigwood NL, Montefiori D, et al. High specific infectivity of plasma virus from the pre-ramp-up and ramp-up stages of acute simian immunodeficiency virus infection. *J Virol.* 2009; 83(7):3288–97. doi: [10.1128/JVI.02423-08](#) PMID: [19129448](#); PubMed Central PMCID: PMC2655556.
54. Macey RI, Oster GF. Berkeley Madonna, version 8.3.18.: Berkeley CA: University of California at Berkeley; 2001.
55. Bates DM, Watts DG. Nonlinear regression analysis: Its applications. New York: Wiley; 1988.
56. Efron B, Tibshirani RJ. An introduction to the bootstrap New York: Chapman & Hall/CRC; 1998.
57. El-Hage N, Bruce-Keller AJ, Knapp PE, Hauser KF. CCL5/RANTES gene deletion attenuates opioid-induced increases in glial CCL2/MCP-1 immunoreactivity and activation in HIV-1 Tat-exposed mice. *J Neuroimmune Pharmacology* 2008; 3(4):275–85. Epub 2008/09/26. doi: [10.1007/s11481-008-9127-1](#) PMID: [18815890](#); PubMed Central PMCID: PMC2722754.
58. Kitai R, Zhao ML, Zhang N, Hua LL, Lee SC. Role of MIP-1beta and RANTES in HIV-1 infection of microglia: inhibition of infection and induction by IFNbeta. *J Neuroimmunology.* 2000; 110(1–2):230–9. Epub 2000/10/12. PMID: [11024554](#).
59. Sasseville VG, Smith MM, Mackay CR, Pauley DR, Mansfield KG, Ringler DJ, et al. Chemokine expression in simian immunodeficiency virus-induced AIDS encephalitis. *Amer J Pathol.* 1996; 149(5):1459–67. Epub 1996/11/01. PMID: [8909235](#); PubMed Central PMCID: PMC1865261.
60. Cornwell WD, Lewis MG, Fan X, Rappaport J, Rogers TJ. Effect of chronic morphine administration on circulating T cell population dynamics in rhesus macaques. *J Neuroimmunol.* 2013; 265(1–2):43–50. doi: [10.1016/j.jneuroim.2013.09.013](#) PMID: [24090653](#); PubMed Central PMCID: PMC3852163.
61. Ho DD, Huang Y. The HIV-1 vaccine race. *Cell.* 2002; 110(2):135–8. Epub 2002/08/02. PMID: [12150921](#).
62. Ribeiro RM, Dixit NM, Perelson AS. Modelling the in vivo growth rate of HIV: implications for vaccination. In: Paton R, McNamara LA, editors. Multidisciplinary approaches to theory in medicine. Amsterdam, Netherland: Elsevier; 2006.
63. Louie M, Hogan C, Di Mascio M, Hurley A, Simon V, Rooney J, et al. Determining the relative efficacy of highly active antiretroviral therapy. *J Infect Dis.* 2003; 187(6):896–900. doi: [10.1086/368164](#) PMID: [12660935](#).
64. Miyagi T, Chuang LF, Doi RH, Carlos MP, Torres JV, Chuang RY. Morphine induces gene expression of CCR5 in human CEMx174 lymphocytes. *The Journal of biological chemistry.* 2000; 275(40):31305–10. Epub 2000/07/11. doi: [10.1074/jbc.M001269200](#) PMID: [10887175](#).
65. Ribeiro RM, Qin L, Chavez LL, Li D, Self SG, Perelson AS. Estimation of the initial viral growth rate and basic reproductive number during acute HIV-1 infection. *J Virol.* 2010; 84(12):6096–102. Epub 2010/04/02. doi: [10.1128/JVI.00127-10](#) PMID: [20357090](#); PubMed Central PMCID: PMC2876646.